MATTER: International Journal of Science and Technology
ISSN 2454-5880

Bello Mary et al., 2022

Volume 8, pp. 153-175

Received: 29th June 2021

Revised: 14th July 2022, 21st July 2022, 1st August 2022

Accepted: 02nd August 2022

Date of Publication: 05th August 2022

DOI- https://doi.org/10.20319/mijst.2022.8.153175

This paper can be cited as: Olubunmi, B. M., Minjun, P., & Genglei, X. (2022). The Effects of System Parameters on Inception of Flashing using Relap5. MATTER: International Journal of Science and Technology, 8, 153-175.

THE EFFECTS OF SYSTEM PARAMETERS ON THE INCEPTION OF FLASHING USING RELAP5

Bello Mary Olubunmi
M.Sc., College of Nuclear Science and Technology, Harbin Engineering University, Harbin, 150001, China
marybello@hrbeu.edu.cn

Peng Minjun
Prof., College of Nuclear Science and Technology, Harbin Engineering University, Harbin, 150001, China
heupmj@hrbeu.edu.cn

Xia Genglei
PhD, College of Nuclear Science and Technology, Harbin Engineering University, Harbin, 150001, China
xiagenglei@163.com

Abstract

Natural circulation systems (NCS) are prone to instabilities, they are more unstable compared to forced circulation systems as a result of the low driving head and nonlinearity of the system. Flashing instability is prominent in these systems at low pressure due to the presence of a long nonheated riser to enhance the driving force. RELAP5 code has been identified as one of the Best Estimate (BE) codes used in the analysis of the systems. The studies by different authors showed that the effects of system parameters on instability generally have gained the attention of

researchers in recent years. However, these studies have not discussed how these parameters prevent or enhance the commencement of flashing instability. This we sought to achieve in this work, by zeroing in on the inception of flashing instability, by comparing what happened at different heat fluxes. The objective of this work is to investigate the effects of system parameters on the inception of flashing instability in a natural circulation system using the RELAP5 code. With the increase in inlet subcooling and height of the riser, flashing moved to the outlet of the riser, stabilizing the system. However, an opposite effect was observed with an increase in the inlet resistance.

Keywords

Inlet Resistance, Inlet Subcooling, Natural Circulation, Nodalization, Oscillation

---

1. Introduction

Natural circulation systems (NCS) are prone to different types of instabilities. Though forced circulation systems also experience instabilities, natural circulation systems are more unstable as a result of the low driving head and nonlinearity of the system. Any little disturbance in the driving head affects the flow which leads to instability. Instabilities can lead to adverse effects in nuclear systems including mechanical damage and problems with control systems.

Flashing instability occurs due to the presence of nucleation sites along the wall of the system (Fraser & Abdelmessih, 2002). It is prominent in natural circulation systems at low pressure as a result of the large hydrostatic pressure drop induced by the long nonheated riser employed to enhance the driving force. RELAP5 code has been identified as one of the Best Estimate (BE) codes used in the analysis of natural circulation systems. As such, several authors have researched to validate the simulation of flashing-induced instability and factors affecting it using the RELAP5 code.

1.1. Theory/Concept of Study

The RELAP5 code uses a partially implicit numerical scheme for a two-phase system. The code solves continuity equations for mass, energy, and momentum.

1.1.1. Mass Equations

The mass continuity equations are given below:

$$\frac{\partial}{\partial t}\left(\alpha_g \rho_g\right) + \frac{1}{A}\frac{\partial}{\partial x}\left(\alpha_g \rho_g v_g A\right) = \Gamma_g \tag{1}$$

$$\frac{\partial}{\partial t}\left(\alpha_f \rho_f\right) + \frac{1}{A}\frac{\partial}{\partial x}\left(\alpha_f \rho_f v_f A\right) = \Gamma_f \tag{2}$$

Where the liquid generation term is negative of the vapour generation term i.e.

$$\Gamma_f = -\Gamma_g \tag{3}$$

The vaporization term is the sum of the heat transfer at the interface and the wall heat transfer, expressed as:

$$\Gamma_g = \Gamma_{ig} + \Gamma_w \tag{4}$$

Each of these processes includes interface heat transfer effects derived from energy balance considerations at the interface.

1.1.2. Momentum Equations

The phasic momentum equations used are in the expanded form in terms of momenta per unit volume using the phasic primitive velocity variables v_g and v_f. The spatial variation of momentum term is expressed in terms of v_g^2 and v_f^2. This type of expression used has the benefit of the momentum equation reducing to Bernoulli's equations for steady, incompressible and frictionless flow. For the gas phase, the equation is:

$$\alpha_g\rho_g A\frac{\partial v_g}{\partial t} + \frac{1}{2}\alpha_g\rho_g A\frac{\partial v_g^2}{\partial x} = -\alpha_g A\frac{\partial P}{\partial x} + \alpha_g\rho_g B_x A - \left(\alpha_g\rho_g A\right)FWG \bullet v_g - \Gamma_g A\left(v_{gi} - v_g\right) - \left(\alpha_g\rho_g A\right)FIG \bullet \left(v_g - v_f\right) - C\alpha_g\alpha_f\rho_m A[\frac{\partial\left(v_g - v_f\right)}{\partial t} + v_f\frac{\partial v_g}{\partial x} + v_g\frac{\partial v_f}{\partial x} \tag{5}$$

For the liquid phase, the equation is:

$$\alpha_f\rho_f A\frac{\partial v_f}{\partial t} + \frac{1}{2}\alpha_f\rho_f A\frac{\partial v_f^2}{\partial x} = -\alpha_f A\frac{\partial P}{\partial x} + \alpha_f\rho_f B_x A - \left(\alpha_f\rho_f A\right)FWF \bullet v_f - \Gamma_g A\left(v_{fi} - v_f\right) - \left(\alpha_f\rho_f A\right)FIF \bullet \left(v_f - v_g\right) - C\alpha_f\alpha_g\rho_m A[\frac{\partial\left(v_f - v_g\right)}{\partial t} + v_g\frac{\partial v_f}{\partial x} + v_f\frac{\partial v_g}{\partial x} \tag{6}$$

The force terms on the right-hand sides of equations (5) and (6) are, respectively, the pressure gradient, the body force (i.e. gravity and pump head), wall friction, momentum transfer as a result of interface mass transfer, interface frictional drag and force as a result of virtual mass. The terms FWG and FWF are part of the wall frictional drag, which are linear in velocity and are products of the friction coefficient, the frictional reference area per unit volume and the magnitude

of the fluid bulk velocity. The interfacial velocity in the interface momentum transfer term is the unit momentum with which phase appearance or disappearance happens. The coefficients FIG and FIF are part of the interface frictional drag, two different models (drift flux and drag coefficient) are used for the interface friction drag, which is dependent on the flow regime.

1.1.3. Energy Equations

The phasic energy equations are:

$$\frac{\partial}{\partial t}\left(\alpha_g \rho_g U_g\right) + \frac{1}{A}\frac{\partial}{\partial t}\left(\alpha_g \rho_g U_g v_g A\right) = -P\frac{\partial \alpha_g}{\partial t} - \frac{P}{A}\frac{\partial}{\partial t}\left(\alpha_g v_g A\right) + Q_{wg} + Q_{ig} + \Gamma_{ig} h_g^* + \Gamma_w h_g' + DISS_g \quad (7)$$

$$\frac{\partial}{\partial t}\left(\alpha_f \rho_f U_f\right) + \frac{1}{A}\frac{\partial}{\partial t}\left(\alpha_f \rho_f U_f v_f A\right) = -P\frac{\partial \alpha_f}{\partial t} - \frac{P}{A}\frac{\partial}{\partial t}\left(\alpha_f v_f A\right) + Q_{wf} + Q_{if} + \Gamma_{ig} h_f^* + \Gamma_w h_f' + DISS_f \quad (8)$$

In equations (7) and (8), Q_{wg} and Q_{wf} are the phasic wall heat transfer rate per unit volume. These phasic wall heat transfer rates satisfy the equation:

$$Q = Q_{wg} + Q_{wf} \quad (9)$$

Where Q is the total wall heat transfer rate to the fluid per unit volume.
The addition of equations (7) and (8) gives the mixture energy equation, this needed the interface transfer terms to add up to zero, that is

$$Q_{ig} + Q_{if} + \Gamma_{ig}\left(h_g^* - h_f^*\right) + \Gamma_w\left(h_g' - h_f'\right) = 0 \quad (10)$$

The interface heat transfer terms, $Q_{ig}\ and\ Q_{if}$, are made up of two parts: interface heat transfer in the bulk, Q_{ig}^B and Q_{if}^B and the interface heat transfer in the thermal boundary layer near the wall, Q_{ig}^W and Q_{if}^W.

The two parts are additive:

$$Q_{ig} = Q_{ig}^B + Q_{ig}^W \quad (11)$$

And

$$Q_{if} = Q_{if}^B + Q_{if}^W \quad (12)$$

The bulk interface heat transfer is at the vapour-liquid interface in the bulk. This constitutes thermal energy exchange between the fluid interface (at the saturation temperature T^S corresponding to the total pressure P) and the bulk fluid state.

For vapour, the bulk interface heat transfer is given by:

$$Q_{ig}^{B} = H_{ig}(T^S - T_g) \tag{13}$$

Where H_{ig} is the vapour interface heat transfer coefficient per unit volume and T_g is the vapour temperature.

For liquid, the bulk interface heat transfer is given by:

$$Q_{if}^{B} = H_{if}(T^S - T_f) \tag{14}$$

Where H_{if} is the liquid interface heat transfer coefficient per unit volume and T_f is the liquid temperature.

Putting equations (13) and (14) into equations (11) and (12),

$$Q_{ig} = H_{ig}(T^S - T_g) + Q_{ig}^{W} \tag{15}$$

$$Q_{if} = H_{if}(T^S - T_f) + Q_{if}^{W} \tag{16}$$

Equation (10) requires the bulk interface energy exchange terms and the near wall interface energy exchange terms to add up to zero individually:

$$H_{ig}(T^S - T_g) + H_{if}(T^S - T_f) + \Gamma_{ig}(h_g^* - h_f^*) = 0 \tag{17}$$

And

$$Q_{ig}^{W} + Q_{if}^{W} + \Gamma_w(h_g' - h_f') = 0 \tag{18}$$

And as it is supposed that vapour occurs at saturation, then $Q_{ig}^{W} = 0$ for boiling processes in the boundary level close to the wall. Solution of Equation (18) then gives the interface vaporization rate at the boundary level close to the walls:

$$\Gamma_w = \frac{-Q_{if}^{W}}{h_g' - h_f'} \tag{19}$$

In the same vein, as it is supposed that liquid occurs at saturation, then $Q_{if}^{W} = 0$ for condensation processes in the boundary level close to the wall. Solution of Equation (18) then gives the interface condensation rate at the boundary level close to the walls:

$$\Gamma_w = \frac{-Q_{ig}^{W}}{h_g' - h_f'} \tag{20}$$

When Equations (19) and (20) are solved for Q_{if}^{W} and Q_{ig}^{W} and the terms are inserted into Equations (15) and (16), the interface energy transfer terms, Q_{ig} and Q_{if}, become:

$$Q_{ig} = H_{ig}(T^S - T_g) - (\frac{1-\varepsilon}{2})\Gamma_w(h'_g - h'_f) \quad (21)$$

And

$$Q_{if} = H_{if}(T^S - T_f) - (\frac{1+\varepsilon}{2})\Gamma_w(h'_g - h'_f) \quad (22)$$

ε =1 for boiling in the boundary level close to the wall;

ε = -1 for condensation in the boundary level close to the wall.

Solving Equation (10) gives the interface vaporization (or condensation) rate in the bulk fluid.

$$\Gamma_{ig} = -\frac{Q_{ig} + Q_{if}}{h^*_g - h^*_f} - \Gamma_w \frac{(h'_g - h'_f)}{h^*_g - h^*_f} \quad (23)$$

And on inserting Equations (21) and (22), it becomes:

$$\Gamma_{ig} = -\frac{H_{ig}(T^S - T_g) + H_{if}(T^S - T_f)}{h^*_g - h^*_f} \quad (24)$$

Inserting Equation (24) into Equation (4) gives the total interface mass transfer.

$$\Gamma_g = -\frac{H_{ig}(T^S - T_g) + H_{if}(T^S - T_f)}{h^*_g - h^*_f} + \Gamma_w \quad (25)$$

2. Literature Review

Previous work on instability started with the excellent work of (Boure, Bergles, & Tong, 1973) and (Fukuda & Kobori, 1979) with recent work by (Ruspini, Marcel, & Clausse, 2014), (Durga Prasad, Pandey, & Kalra, 2007) and (Kakac & Bon, 2008).

(Khandelwal & Ishii, 2021) carried out an analytical study of instability induced by flashing in natural circulation systems. They discovered that theoretically flashing instabilities were not affected by inlet and exit restrictions due to strong integration of flow velocity and pressure drop in the system. (Hou et al., 2021) studied the steady-state response of flashing-driven open natural circulation system. They noted that the flow rate increased just a bit with an increase in riser length during the flashing flow while an increase in the diameter of the riser led to a considerable increase in the flow.

(Zhao, Peng, Xu, & Xia, 2020) studied flashing-induced instability in a natural circulation system and the various oscillation patterns observed due to variations in system parameters. Also,

(Guo, Sun, Wang, & Yu, 2015) observed various oscillation behaviour resulting from flashing and how changes in system parameters affected the instability. (Kozmenkov, Rohde, & Manera, 2012) carried out an analysis to validate RELAP5 code in modelling flashing-induced instabilities using results from experiments carried out on the CIRCUS facility developed in the Netherlands and observed that the code gave results that were in good agreement with the experimental results. The effects of changes in system parameters on the stability were observed by modelling in detail, the various components of the facility including the heat exchanger, steam dome and buffer vessel, which enhanced the accuracy of the results obtained.

Furthermore, (Shi & Ishii, 2017) carried out a frequency domain analysis using the drift flux model and a developed flashing model to determine the stability boundary of flashing instability and DWO of a modular reactor. Using stability maps developed from dimensionless numbers, they discovered that the boundary predicted by the model for flashing instability differed from that obtained experimentally. In the experimental results, the flashing boundary was located above the zero-quality line while in the analytical result; it was below the zero-quality line. This was attributed to the thermal equilibrium assumed in the model. Non-thermal equilibrium combined with frequency domain analysis was put forward for future work.

(Hou, Sun, & Lei, 2017) studied the ability of RELAP5 code to simulate the thermal-hydraulic behaviour of open natural circulation. They observed that the code produced results that agreed well with experiments in describing flashing instability and also noticed how the parameters affected the flashing instability. (Hagen & Stekelenburg, 1997) observed some unstable characteristics at certain conditions and at low power and pressure in the experiment they carried out at the Dutch natural circulation BWR Dodewaard facility. (Sawai, Kaji, Nakanishi, & Yamaguchi, 1999) carried out an analysis using the Homogeneous Equilibrium Model (HEM) at low pressure. However, no pressure changes along the wall of the system were considered which were necessary for unstable behaviour in the system, but some flow transitions observed in the analysis could not be confirmed experimentally afterwards by other authors.

(Inada, Furuya, & Yasuo, 2000) also used the HEM to analyze a boiling circulation system and the stability boundaries obtained agreed fairly well with the experimental results. (Cheung, Shiralkar, & Marquino, 2005) employed the TRACG code in analyzing the start-up procedure of ESBWR and observed that the main instability at startup was flashing instability. (Lakshmanan &

Pandey, 2009) also noted that flashing instability was one of the oscillations observed in the startup of a test facility and its natural circulation reactor prototype.

2.1. Problem Identification and Objective of Study

The studies by different authors enumerated above showed that the effects of system parameters on instability generally have gained the attention of researchers in recent years. However, these studies have not discussed how these parameters prevent or enhance the commencement of flashing instability. This we sought to achieve in this work, by zeroing in on the inception of flashing instability, and comparing what happened at different heat fluxes.

The objective of the present work is, therefore, to investigate the effects of system parameters on the inception of flashing instability in a natural circulation system using the RELAP5 code. In section 2, we discuss the facility and RELAP5 nodalization. The results and discussions are given in section 3 and the conclusions in section 4.

3. Investigation Approach

RELAP5 code, a transient analysis code, was used to carry out the work done in this paper. This was used to simulate a natural circulation test facility to study flashing instability and the effects the system parameters have on it.

3.1. Natural Circulation Test Facility

The natural circulation test facility was developed for the Purdue Novel Modular Reactor with an electric output of 50MWe. It was to study the thermal-hydraulic behaviour of the system at low temperature and low pressure. The test facility is made up of the heating section, which consists of four heaters, the pre-heating section, the riser, separator, steam dome, condenser and downcomer. The preheating section is to regulate correctly the inlet temperature of the fluid. The heater power is 20kW and it has two heat exchangers in a supplementary pipeline which are employed for the startup procedure but disconnected during the experiments. The details of the facility and the instrumentation are given in (Ishii et al., 2015) and (Shi et al., 2015) and the schematic diagram is shown in Figure 1(a).

3.2. RELAP5 Model and Nodalization

The light water reactor (LWR) transient analysis code, RELAP5 code (Co, 1995), was developed at the Idaho National Engineering Laboratory (INEL) for the U.S. Nuclear Regulatory Commission (NRC). RELAP5 code is a highly generic code that, in addition to calculating the

behaviour of a reactor coolant system during a transient, can be used for simulation of a wide variety of hydraulic and thermal transients in both nuclear and non-nuclear systems involving mixtures of steam, water, noncondensable and solutes.

The RELAP5/MOD 4.0 version of the code was used in the simulation, the nodalization adopted is shown in Figure 1(b). Pipes and branches were used to represent the various components of the facility, joined by single junctions. The core was represented by the first eleven volumes of pipe 108 and the heat structure 1108H provided the heating power, the remaining twenty volumes of pipe 108 represented the riser to show the phenomena occurring in the riser accurately. The preheater was represented with pipe 106 and its function was enhanced by connecting an extra heat exchange loop, 200 series, to it. This helped to accurately keep the inlet temperature at the desired value. The lower plenum (containing the unheated part of the electric heater) was modelled with a branch which was used to control the inlet flow resistance of the system. The downcomer was modelled with pipe 100 having ten volumes with a heat exchange loop, 400 series, also connected to the first two volumes to maintain the inlet temperature. A big heat transfer area was set between pipe 402 and volumes 10001 and 10002 to ensure the desired inlet temperature was achieved. The steam dome was simulated with branch 118. The pressure of the system was set by the time-dependent volume connected to the steam dome.

The operation conditions of the facility (shown in Table 1) were used as input parameters in the RELAP5 code simulation to ensure the model truly represents the physical attributes of the test facility.

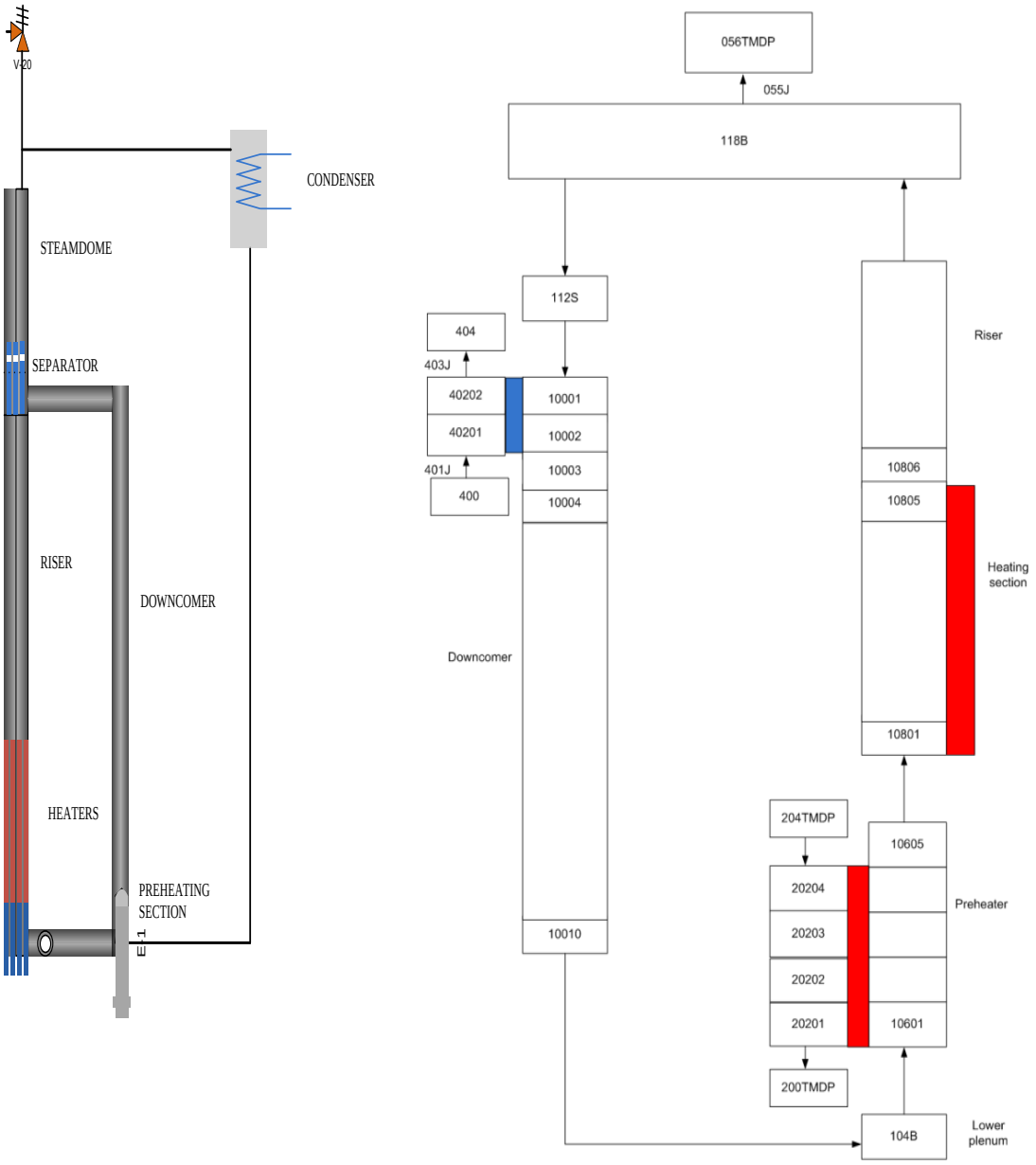

(a) (b)

Figure 1: *(a) Schematic of the Natural Circulation Test Facility (b) Nodalization diagram for the facility (Ishii et al., 2015)*

Table 1: *Operating Parameters of the Test Facility*

Equipment	Value (mm)
Test Apparatus	
Total height	7000.00
Wall thickness	3.05
Heating section	
Heating length	1130.00
Tube Inner diameter	82.80
Hydraulic diameter	23.00
Top of heater	1950.00
Riser	
Tube Inner diameter	82.80
Top of riser	5260.00
Downcomer	
Tube inner diameter	54.80

*(**Source:** Shi et al., 2015 - Table 3)*

4. Results and Discussion

In this work, the nodalization sensitivity was first carried out, after which the oscillations observed at different pressures were analysed. The effects of the system parameters on flashing were then studied at different heat fluxes, pressures and temperatures.

4.1. Nodalization Sensitivity

Previous authors have shown that RELAP5 results are affected by the nodalization employed in simulation (Mangal, Jain, & Nayak, 2012). As a result of this, the nodalization sensitivity was carried out using a different number of volumes for the major components as shown in Table 2. Figure 2 shows the result of the three different nodalizations: Nodalization 1, Nodalization 2 and Nodalization 3. From the graph, we observed that the results from the three nodalization schemes were similar. Therefore, Nodalization 1 was employed for this work as it gives equivalent results to the others in the shortest calculation time.

Table 2: *Number of volumes for major components*

Component	Nodalization 1	Nodalization 2	Nodalization 3
Core	11	11	11
Riser	20	40	60
Downcomer	10	20	40

Total	41	71	111

*(**Source:** Self-compiled)*

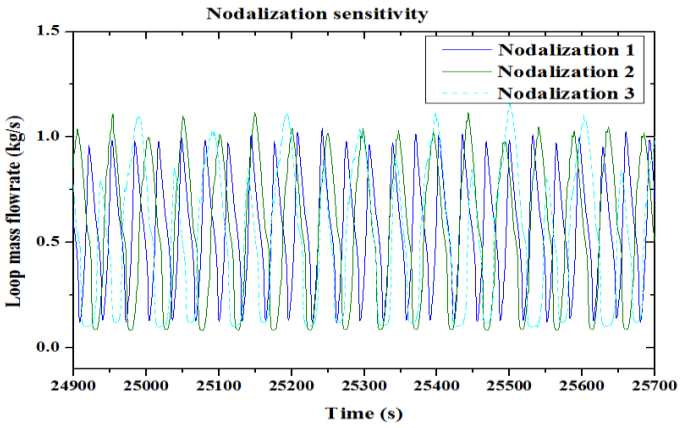

(**Figure 2**: *Nodalization sensitivity)*

*(**Source:** Self-compiled)*

4.2. Oscillations at Different Pressures

RELAP5 code showed clearly the suppression of instability at higher pressures as seen in Figure 3(b) when compared with Figure 3(a). This was also observed by other authors: (Masuhara, Ustuno, Bessho, Yokomizo, & Fukahori, 1993) and (Furuya, Inada, & van der Hagen, 2005). Instability is more prominent at lower pressure due to increased thermal non-equilibrium at this pressure (Shi & Ishii, 2017).

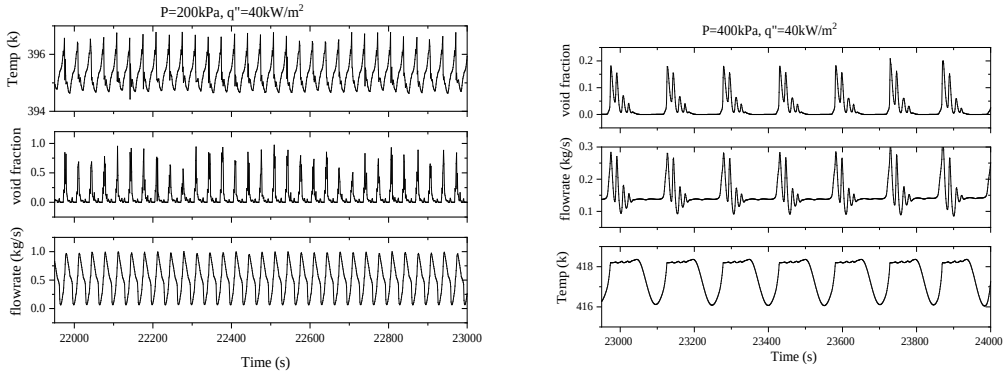

(a) (b)

Figure 3: *(a)Instability at P=200kPa, q"=40kW/m^2 (b) Instability at P=400kPa, q"=40kW/m^2*

*(**Source:** Self-compiled)*

4.3. Effect of Inlet Subcooling on Flashing Instability

Having established that flashing was more pronounced at lower pressure in the last section, the effect of inlet subcooling on flashing was studied at different heat fluxes in this section. The effect on the onset of flashing was observed as shown below.

- Inlet subcooling of 10^0C

Figures 4(a) - (c) showed the results obtained at an inlet subcooling of 10^0C observed at different heat fluxes:

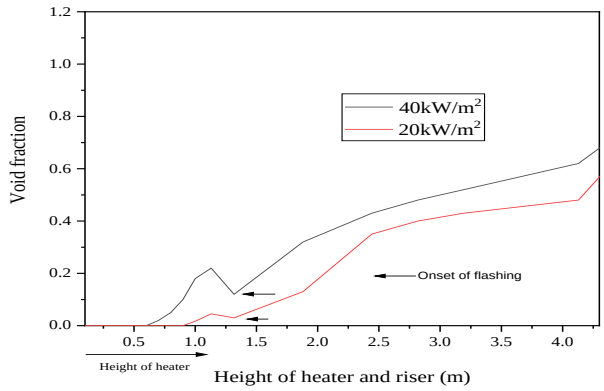

Fig. 4(a): Flashing observed at P=200kPa; inlet subcooling =10k, q" = 40kW/m^2 and 20kW/m^2

*(**Source:** Self-compiled)*

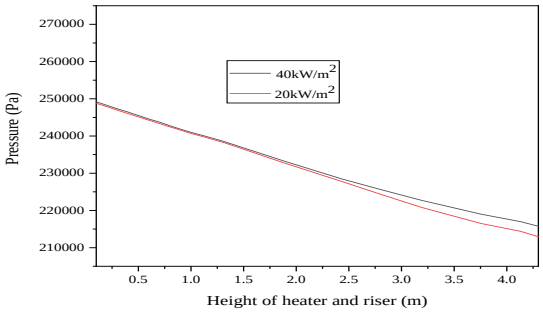

(b)

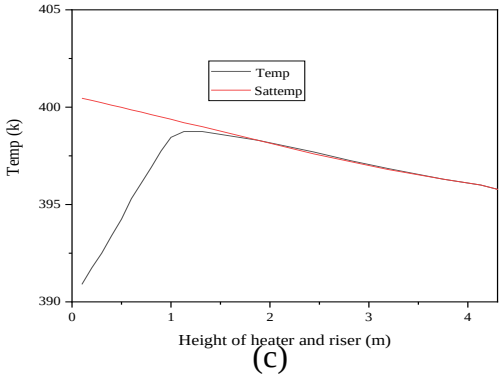

(c)

(**Figure 4**: *(b) Pressure; and (c) Temperature at P=200kPa; inlet subcooling =10k)*

*(**Source:** Self-compiled)*

The onset of flashing was at the inlet of the riser for both heat fluxes as shown in Figure 4(a). A higher void fraction was observed at the higher heat flux showing an increased flashing

process at higher heat flux due to a rise in the energy of the water molecules at this level. Flashing was observed when the temperature exceeded the saturated temperature. Also, the saturated temperature decreased as the pressure as seen in Figure 4(b). Subcooled boiling was observed at the outlet of the heater as well.

- Inlet subcooling of 20k

Figures 5 (a) - (b) showed the results obtained at an inlet subcooling of 20k.

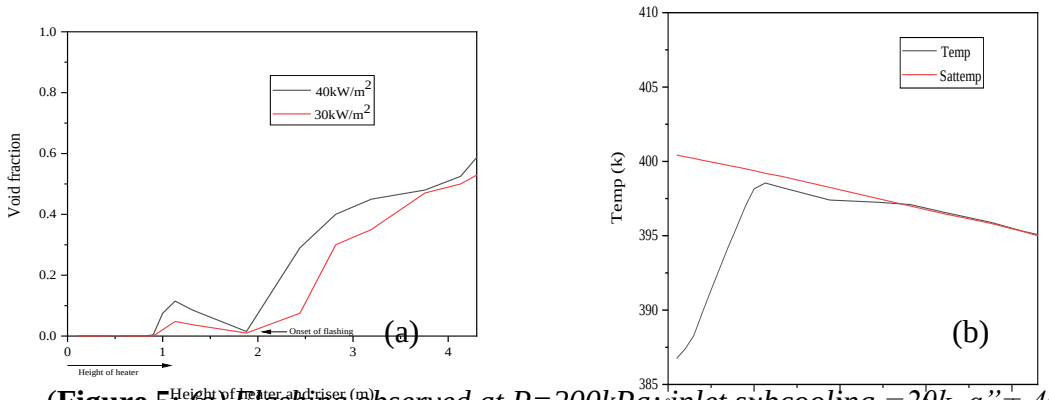

(**Figure 5**: *(a) Flashing observed at P=200kPa; inlet subcooling =20k, q''= 40kW/m^2 and 30kW/m^2 (b)Temperature at P=200kPa; inlet subcooling =20k)*

*(**Source:** Self-compiled)*

The onset of flashing moved upwards towards the centre of the riser for both heat fluxes as shown in Figure 5(a). An increase in inlet subcooling moved the flashing upwards towards the outlet of the riser. Also, the saturated temperature decreased as the pressure, and subcooled boiling as well was observed at the outlet of the heater.

- Inlet subcooling of 30k

Figures 6 (a) - (b) showed the results obtained at an inlet subcooling of 30k

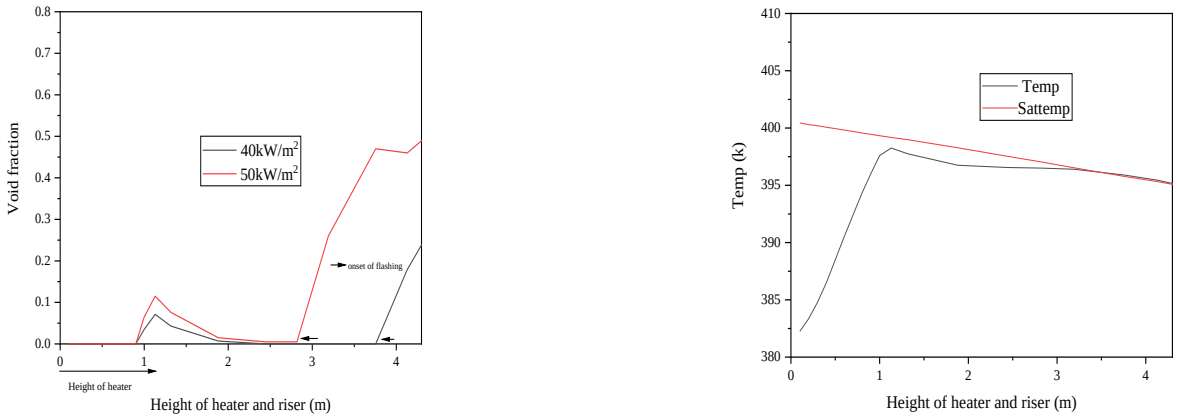

(**Figure 6**: *(a) Flashing observed at P=200kPa; inlet subcooling=30k, q"= 40kW/m^2 and 50kW/m^2 (b) Temperature at P=200kPa; inlet subcooling =30k)*

*(**Source:** Self-compiled)*

The onset of flashing moved to the outlet of the riser. Also, the saturated temperature decreased as the pressure. Subcooled boiling was observed at the outlet of the heater. The inlet subcooling affects the point of inception of flashing in all the conditions examined. As the inlet subcooling increased, the onset of flashing moved to the outlet of the riser. (Fraser & Abdelmessih, 2002) also made this observation in their experiment.

4.4. Effect of the height of the riser on flashing Instability

The effect of the different heights of the riser on flashing was studied at a heat flux of 40kW/m^2 and inlet subcooling of 30k in this section. The effect on the onset of flashing was observed as shown below.

(a) Riser height of 4.5m

Figures 7 (a) - (c) showed the results obtained at a riser height of 4.5m:

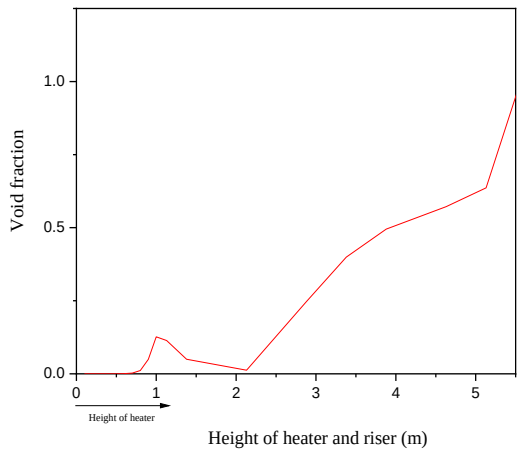

(**Figure7**: (*a) Flashing observed at riser height of 4.5m)*

*(**Source:** Self-compiled)*

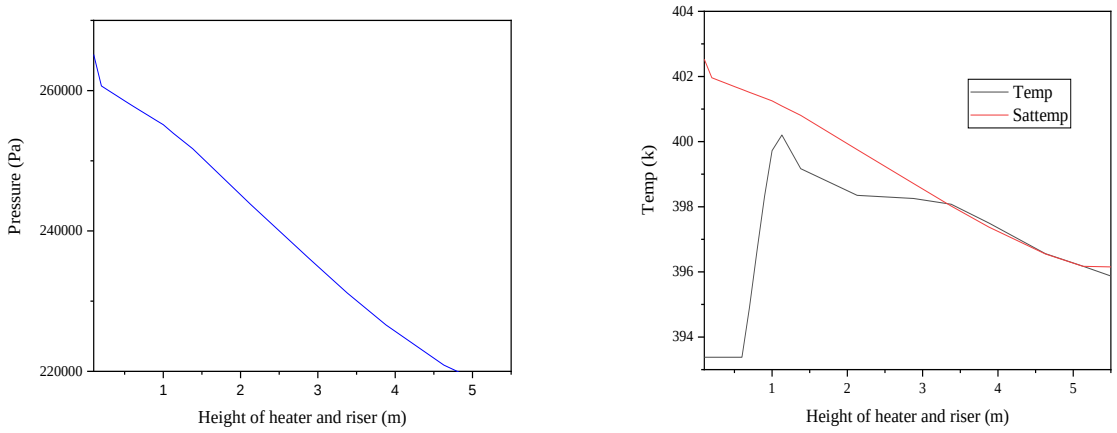

(b) (c)

(**Figure 7**: (*b) Pressure and (c) Temperature observed at riser height of 4.5m)*

*(**Source:** Self-compiled)*

The onset of flashing was observed at the inlet of the riser while subcooled boiling was also observed at the outlet of the heater as seen in Figure 7(a). Saturated temperature decreased as the pressure in Figure 7 (b) and a step-wise decrease was noticed in the temperature of the system in Figure 7 (c).

- Riser height of 6.5m

Figures 8 (a)-(c) showed the results obtained at a riser height of 6.5m:

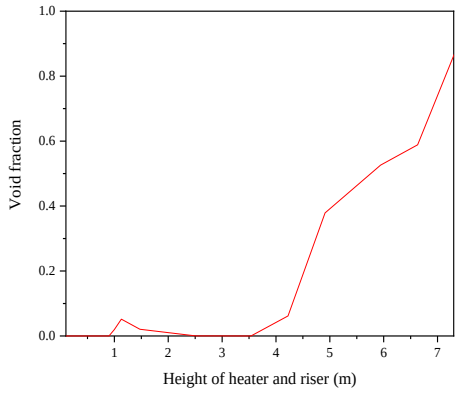

(**Figure 8**: *(a) Flashing observed at riser height of 6.5m)*

*(**Source:** Self-compiled)*

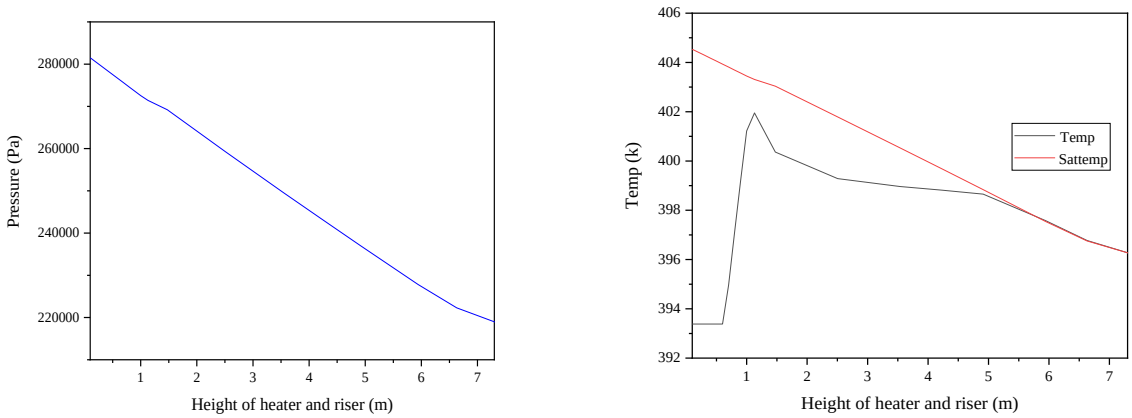

(b) (c)

Figure 8: *(b) Pressure and (c) Temperature observed at riser height of 6.5m*

*(**Source:** Self-compiled)*

The onset of flashing moved upwards towards the centre of the riser with little subcooled boiling observed at the outlet of the heater in Figure 8 (a)

(b) Riser height of 8.5m

Figure 9 (a) showed the result obtained at a riser height of 8.5m

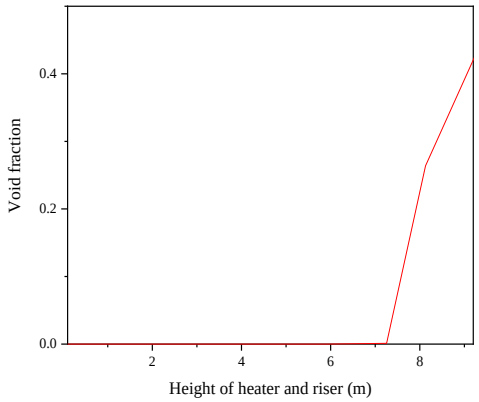

Figure 9: (*a) Flashing observed at riser height of 8.5m*

*(**Source:** Self-compiled)*

The onset of flashing was observed at the outlet of the riser with no subcooled boiling observed as seen in Figure 9(a). Boiling was suppressed at the outlet of the heater due to an increase in the hydrostatic pressure at the outlet of the heater leading to an increase in the local saturation temperature. The height of the riser affected the point of inception of flashing in all the conditions examined. As the height of the riser increased, the onset of flashing moved to the outlet of the riser and boiling was suppressed. This showed that the effect of flashing became more pronounced as the length of the riser increased as observed by (Lakshmanan & Pandey, 2009). They noted that the flashing in the prototype was more pronounced than what was observed in the model as a result of the large variation in saturation temperature due to the height of the riser in the prototype which was four times that of the model. The increase in inlet subcooling and the increase in the height of the riser have similar effects on the onset of flashing as observed in the system

4.5. Effect of inlet resistance on flashing Instability

The effect of the different inlet resistances on flashing was studied at a heat flux of 40kW/m^2 and inlet subcooling of 30k in this section. The effect on the onset of flashing was observed as shown below.

- Inlet resistance of 10

Figure 10 shows the result obtained with an inlet resistance of 10

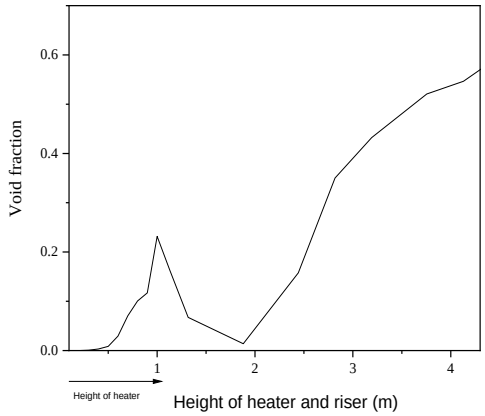

Figure 10: *Flashing observed at inlet resistance of 10*

*(**Source:** Self-compiled)*

The onset of flashing was towards the centre of the riser with an inlet resistance of 10.

- Inlet resistance of 50

Figure 11 shows the result obtained at an inlet resistance of 50

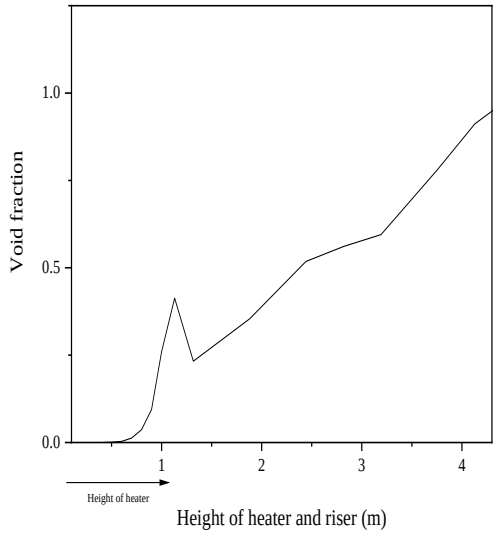

(**Figure 11***: Flashing observed at inlet resistance of 50)*

***(Source:** Self-compiled)*

The onset of flashing occurred at the inlet of the riser for inlet resistance of 50.

- Inlet resistance of 100

Figure 12 showed the result obtained with an inlet resistance of 100

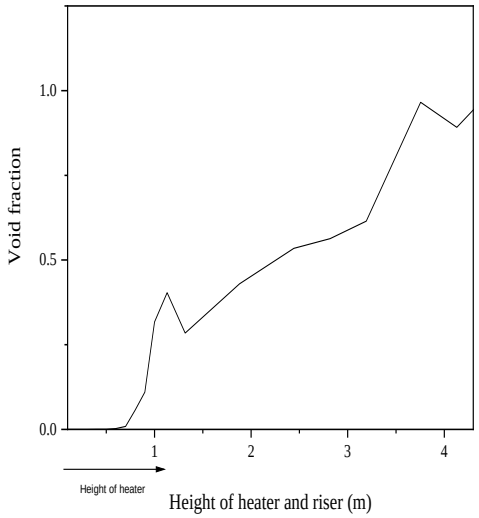

(**Figure 12**: *Flashing observed at inlet resistance of 100)*

*(**Source:** Self-compiled)*

The onset of flashing moved to the inlet of the riser with an increase in inlet resistance as seen with the inlet resistance of 50 and 100 in Figure 11 and Figure 12 making the system unstable. This was also the conclusion of (Marcel, Rohde, & Van Der Hagen, 2009) in the experiment carried out on the CIRCUS facility.

While with an increase in inlet subcooling and height of the riser, flashing moved to the outlet of the riser, stabilizing the system, an opposite effect was observed with an increase in the inlet resistance.

5. Conclusions

Natural circulation systems (NCS) are prone to different types of instabilities. Flashing instability occurs due to the presence of nucleation sites along the wall of the system, it is prominent in natural circulation systems at low pressure. The test facility was developed for the Purdue Novel Modular Reactor to study the thermal-hydraulic behaviour of the system at low temperature and low pressure. RELAP5 code was used to simulate flashing instability at different system parameters for the facility. The code simulated the instability at different inlet pressures and also showed the suppression of flashing at higher pressure. Subcooled boiling was also observed in the heated section of the system.
The effects of system parameters on the onset of flashing were observed to be dependent on the particular parameter being considered. The inlet subcooling and riser height on one hand have similar effects on the onset of flashing which moved to the outlet of the riser with an increase in inlet subcooling and also with an increase in riser height which stabilized the system. On the other hand, the onset of flashing moved to the inlet of the riser with an increase in the inlet resistance, making the system more unstable.

5.1 Scope of Future Research

Further work can be carried out on the effects of the height of the downcomer and the diameters of the riser and the downcomer on the onset of flashing and the results compared with studies from other authors.

5.2 Research Limitations

In this work, we did not consider the effects the diameters of the riser and downcomer could have on flashing inception due to time constraints. Also, there are limited studies on how system parameters affect the onset of flashing.

6. Acknowledgments

This work is supported by the National Natural Science Foundation of China (Grant No. 51709067). Zhao Yanan and Xu Yifan are acknowledged for their assistance and support.

REFERENCES

Boure, J. A., Bergles, A. E., & Tong, L. S. (1973). Review of two-phase flow instability. *Nuclear Engineering and Design, 25*(2), 165-192. https://doi.org/10.1016/0029-5493(73)90043-5

Cheung, Y. K., Shiralkar, B. S., & Marquino, W. (2005). Analysis of ESBWR startup in natural circulation. *Proceedings of ICAPP '05 Paper 5484, Seoul, Korea, May 15-19, 2005*.

Co, L. I. T. (1995). *RELAP5/MOD3 code manual: User's guide and input requirements* (Vol. 2).

Durga Prasad, G. V., Pandey, M., & Kalra, M. S. (2007). Review of research on flow instabilities in natural circulation boiling systems. *Progress in Nuclear Energy, 49*(6), 429-451. https://doi.org/10.1016/j.pnucene.2007.06.002

Fraser, D. W. H., & Abdelmessih, A. H. (2002). A study of the effects of the location of flashing inception on maximum and minimum critical two_phase flow rates-Part I - experimental. *Nuclear Engineering and Design, 211*, 1-11. https://doi.org/10.1016/S0029-5493(01)00409-5

Fukuda, K., & Kobori, T. (1979). Classification of two-phase flow instability by density wave oscillation model. *Journal of Nuclear Technology, 16*, 95–108. https://doi.org/10.1080/18811248.1979.9730878

Furuya, M., Inada, F., & van der Hagen, T. H. J. J. (2005). Flashing-induced density wave oscillations in a natural circulation BWR—mechanism of instability and stability map. *Nuclear Engineering and Design, 235*(15), 1557-1569. https://doi.org/10.1016/j.nucengdes.2005.01.006

Guo, X., Sun, Z., Wang, J., & Yu, S. (2015). Simulating investigations on the start-up of the open natural circulation system. *Nuclear Engineering and Design, 289*, 35-48.

https://doi.org/10.1016/j.nucengdes.2015.03.021

Hagen, T. H. J. J. v. d., & Stekelenburg, A. J. C. (1997). The low-power low-pressure flow resonance in a natural circulation cooled boiling water reactor. *177*, 229-238. https://doi.org/10.1016/S0029-5493(97)00196-9

Hou, X., Qiu, J., Sun, Z., Yao, S., He, C., Yang, X., Wang, S., & Yang, Y. (2021). A study on the steady-state flow behavior of the flashing-driven open natural circulation system. *Applied Thermal Engineering, 182,* 115903. https://doi.org/10.1016/j.applthermaleng.2020.115903

Hou, X., Sun, Z., & Lei, W. (2017). Capability of RELAP5 code to simulate the thermal-hydraulic characteristics of open natural circulation. *Annals of Nuclear Energy, 109*, 612-625. https://doi.org/10.1016/j.anucene.2017.06.010

Inada, F., Furuya, M., & Yasuo, A. (2000). Thermo-hydraulic instability of boiling natural circulation loop induced by flashing (analytical consideration). *Nuclear Engineering and Design, 200*, 187-199. https://doi.org/10.1016/S0029-5493(99)00334-9

Ishii, M., Shi, S., Yang, W. S., Wu, Z., Rassame, S., & Liu, Y. (2015). Novel modular natural circulation BWR design and safety evaluation. *Annals of Nuclear Energy, 85*, 220-227. https://doi.org/10.1016/j.anucene.2015.05.009

Kakac, S., & Bon, B. (2008). A Review of two-phase flow dynamic instabilities in tube boiling systems. *International Journal of Heat and Mass Transfer, 51*(3), 399-433. https://doi.org/10.1016/j.ijheatmasstransfer.2007.09.026

Khandelwal, A. K., & Ishii, M. (2021). Two-phase flow instability induced by flashing in natural circulation systems: An analytical approach. *International Journal of Heat and Mass Transfer, 181,* 121890. https://doi.org/10.1016/j.ijheatmasstransfer.2021.121890

Kozmenkov, Y., Rohde, U., & Manera, A. (2012). Validation of the RELAP5 code for the modeling of flashing-induced instabilities under natural-circulation conditions using experimental data from the CIRCUS test facility. *Nuclear Engineering and Design, 243*, 168-175. https://doi.org/10.1016/j.nucengdes.2011.10.053

Lakshmanan, S. P., & Pandey, M. (2009). Analysis of startup oscillations in natural circulation boiling systems. *Nuclear Engineering and Design, 239*(11), 2391-2398. https://doi.org/10.1016/j.nucengdes.2009.06.017

Mangal, A., Jain, V., & Nayak, A. K. (2012). Capability of the RELAP5 code to simulate natural

circulation behavior in test facilities. *Progress in Nuclear Energy, 61*, 1-16. https://doi.org/10.1016/j.pnucene.2012.06.005

Marcel, C. P., Rohde, M., & Van Der Hagen, T. H. J. J. (2009). Experimental and numerical investigations on flashing-induced instabilities in a single channel. *Experimental Thermal and Fluid Science, 33*(8), 1197-1208. https://doi.org/10.1016/j.expthermflusci.2009.08.001

Masuhara, Y., Ustuno, H., Bessho, Y., Yokomizo, O., & Fukahori, T. (1993). *Research on geysering phenomena in the natural circulation BWR*, New York, NY, United States.

Ruspini, L. C., Marcel, C. P., & Clausse, A. (2014). Two-phase flow instabilities: A review. *International Journal of Heat and Mass Transfer, 71*, 521-548. https://doi.org/10.1016/j.ijheatmasstransfer.2013.12.047

Sawai, T., Kaji, M., Nakanishi, S., & Yamaguchi, S. (1999). Stability and non-linear dynamics in natural circulation loop at low pressure condition. *2nd international symposium on Two-phase Modeling and Experimentation, May 23-26, Pisa, Italy*, 363-369.

Shi, S., & Ishii, M. (2017). Modeling of flashing-induced flow instabilities for a natural circulation driven novel modular reactor. *Annals of Nuclear Energy, 101*, 215-225. https://doi.org/10.1016/j.anucene.2016.11.005

Shi, S., Schlegel, J. P., Brooks, C. S., Lin, Y.-C., Eoh, J., Liu, Z., . . . Ishii, M. (2015). Experimental investigation of natural circulation instability in a BWR-type small modular reactor. *Progress in Nuclear Energy, 85*, 96-107. doi: https://doi.org/10.1016/j.pnucene.2015.06.014

Zhao, Y., Peng, M., Xu, Y., & Xia, G. (2020). Simulation investigation on flashing-induced instabilities in a natural circulation system. *Annals of Nuclear Energy, 144*. https://doi.org/10.1016/j.anucene.2020.107561